

## LIN28 Expression in Malignant Germ Cell Tumors Downregulates *let-7* and Increases Oncogene Levels

Matthew J. Murray<sup>1,2</sup>, Harpreet K. Saini<sup>4</sup>, Charlotte A. Siegler<sup>1</sup>, Jennifer E. Hanning<sup>1</sup>, Emily M. Barker<sup>1</sup>, Stijn van Dongen<sup>4</sup>, Dawn M. Ward<sup>1</sup>, Katie L. Raby<sup>1</sup>, Ian J. Groves<sup>1</sup>, Cinzia G. Scarpini<sup>1</sup>, Mark R. Pett<sup>1</sup>, Claire M. Thornton<sup>5</sup>, Anton J. Enright<sup>4</sup>, James C. Nicholson<sup>2</sup>, Nicholas Coleman<sup>1,3</sup>, and on behalf of the CCLG

### Abstract

Despite their clinicopathologic heterogeneity, malignant germ cell tumors (GCT) share molecular abnormalities that are likely to be functionally important. In this study, we investigated the potential significance of downregulation of the *let-7* family of tumor suppressor microRNAs in malignant GCTs. Microarray results from pediatric and adult samples ( $n = 45$ ) showed that *LIN28*, the negative regulator of *let-7* biogenesis, was abundant in malignant GCTs, regardless of patient age, tumor site, or histologic subtype. Indeed, a strong negative correlation existed between *LIN28* and *let-7* levels in specimens with matched datasets. Low *let-7* levels were biologically significant, as the sequence complementary to the 2 to 7 nt common *let-7* seed "GAGGUA" was enriched in the 3' untranslated regions of mRNAs upregulated in pediatric and adult malignant GCTs, compared with normal gonads (a mixture of germ cells and somatic cells). We identified 27 mRNA targets of *let-7* that were upregulated in malignant GCT cells, confirming significant negative correlations with *let-7* levels. Among 16 mRNAs examined in a largely independent set of specimens by quantitative reverse transcription PCR, we defined negative-associations with *let-7e* levels for six oncogenes, including *MYCN*, *AURKB*, *CCNF*, *RRM2*, *MKI67*, and *CI2orf5* (when including normal control tissues). Importantly, *LIN28* depletion in malignant GCT cells restored *let-7* levels and repressed all of these oncogenic *let-7* mRNA targets, with *LIN28* levels correlating with cell proliferation and *MYCN* levels. Conversely, ectopic expression of *let-7e* was sufficient to reduce proliferation and downregulate *MYCN*, *AURKB*, and *LIN28*, the latter via a double-negative feedback loop. We conclude that the *LIN28/let-7* pathway has a critical pathobiologic role in malignant GCTs and therefore offers a promising target for therapeutic intervention. *Cancer Res*; 73(15); 4872–84. ©2013 AACR.

### Introduction

Germ cell tumors (GCT) are clinically and histopathologically complex. They present from early infancy through to late adulthood, occur at both gonadal and extragonadal sites, and comprise diverse histologic subtypes (1). Benign forms show somatic differentiation and are termed teratomas, whereas malignant GCTs are classified into germinomas (a collective term for testicular seminoma, ovarian dysgerminoma, and extragonadal germinoma) and non-germinomatous tumors, the main types of which are yolk sac tumors (YST) and embryonal carcinoma (1).

Although most patients with malignant GCTs have a good prognosis, some patients still have inferior outcomes, and testicular germ cell malignancy remains a leading cause of death in young men (2). Improved understanding of the molecular pathogenesis of malignant GCTs would represent an important step toward developing novel therapeutic agents with favorable toxicity profiles, which may improve survival for patients with high-risk disease and reduce toxicity for low-risk patients. It is particularly important to identify abnormalities that are shared across the diverse spectrum of malignant GCTs, as these are likely to be of fundamental significance in disease pathogenesis.

Using microarray profiling, we previously identified that all 9 members of the *let-7* (*let-7*) microRNA family were significantly underexpressed in pediatric malignant GCTs, when compared with nonmalignant control tissues (3). MicroRNAs regulate gene expression via their 5' seed region (nucleotides at positions 1–8; 1–8 nt), which binds the corresponding seed complementary region (SCR) located predominantly in the 3' untranslated region (3'UTR) of mRNA targets (4). Within the seed, 2 to 7 nt are most critical for binding specificity (5). Importantly, all 9 *let-7* microRNAs share the same 2 to 7 nt seed sequence (GAGGUA) and therefore share mRNA targets containing the 3'UTR SCR "TACCTC."

**Authors' Affiliations:** <sup>1</sup>Department of Pathology, Cambridge University; Departments of <sup>2</sup>Paediatric Oncology and <sup>3</sup>Histopathology, Addenbrooke's Hospital; <sup>4</sup>EMBL European Bioinformatics Institute, Hinxton, Cambridge; and <sup>5</sup>Department of Pathology, Royal Group of Hospitals Trust, Belfast, United Kingdom

**Note:** Supplementary data for this article are available at Cancer Research Online (<http://cancerres.aacrjournals.org/>).

**Corresponding Author:** Matthew J. Murray, Department of Pathology, Cambridge University, Cambridge, United Kingdom. Phone: 44-1223-765066; Fax: 44-1223-333346; E-mail: [mjm16@cam.ac.uk](mailto:mjm16@cam.ac.uk)

doi: 10.1158/0008-5472.CAN-12-2085

©2013 American Association for Cancer Research.

*Let-7* microRNAs are important tumor suppressor genes (6) that regulate cell proliferation (7). The *let-7* microRNA family is negatively regulated by the RNA-binding proteins *LIN28 homolog-A* (*LIN28*) and *LIN28 homolog-B* (*LIN28B*; refs. 8, 9), with *LIN28* depletion resulting in specific increases in all *let-7* family members (8, 10). The LIN28 proteins bind *let-7* primary transcripts (*pri-let-7*) and precursor hairpins (*pre-let-7*), preventing processing by DROSHA and DICER1, respectively (11). Binding of *pre-let-7* by LIN28 occurs through a stem loop motif that includes "GGAG" (12, 13), leading to recruitment of the terminal-uridylyl-transferase (TUTase) ZCCHC11 (10, 12), resulting in *pre-let-7* uridylation and subsequent degradation (14).

*LIN28* can reprogram human somatic cells into pluripotent stem cells, and is a putative cancer stem-cell marker (9, 11, 15). Of note, *LIN28* is expressed at high levels in primordial germ cells (16), believed to be the cell of origin for malignant GCTs (1). Previous studies used immunohistochemistry (17–19) and RNA interference (RNAi; ref. 20) to investigate the expression and some aspects of *LIN28* function in malignant GCTs. Here, we provide the first demonstration that low *let-7* levels in malignant GCTs are directly attributable to *LIN28* expression and are likely to contribute to significant upregulation of important cancer-associated protein-coding genes.

## Materials and Methods

### Tumor samples

Our study received ethical approval from Trent-MREC (ref: 02/4/071) and Cambridge-LREC (ref: 01/128). We analyzed the following tissue samples and datasets:

**Set 1.** Forty-eight samples of pediatric malignant GCTs and nonmalignant controls, which we previously used for global microRNA profiling (3) and for global mRNA profiling, a subset of 21 cases (3). Across the sample set, the controls ( $n = 8$ ) represented fetal yolk sac, fetal ovary, prepubertal testis, postpubertal testis, prepubertal ovary, and postpubertal ovary. These samples contain germ cells, with variable representation of somatic cells (21). One apparent teratoma sample (MT-34) was not included in any subsequent analysis as it was a component of a mixed malignant GCT and clustered with malignant cases on microRNA profiling (3). The remaining 20 samples with matched microRNA and mRNA profiles comprised 17 malignant GCTs (10 YSTs, 6 germinomas, and 1 embryonal carcinoma) and 3 normal gonadal controls (1 pre- and 1 postpubertal testis and 1 postpubertal ovary; ref. 3).

**Set 2.** A published dataset of global mRNA expression profiles of 25 samples from a study of adult testicular malignant GCTs (8 YSTs; 12 germinomas) and controls (5 normal adult testes, containing germ cells and somatic cells). Further details are available in the original publication (22) and our previous study (3).

**Set 3.** Thirty-two samples in which we measured levels of selected mRNAs and microRNAs by quantitative reverse transcription PCR (qRT-PCR). Full details are given in Supplementary Table S1. The malignant GCTs represented 9 YSTs, 9 germinomas, and 3 embryonal carcinomas, with all except 3 being from pediatric patients (< 16 years). In addition, we used 6 malignant GCT cell lines and 5 benign teratomas. Twenty-four of the 32 samples overlapped with set 1 and had previously

been used for microRNA profiling (3). However, only 6 of the 32 had undergone mRNA profiling (3; Supplementary Table S1), enabling set 3 to be used for independent qRT-PCR validation of findings from our mRNA microarray analyses of sets 1 and 2.

When combining sets 1 to 3, our study encompassed a total of 81 samples, comprising 54 different malignant GCTs (31 pediatric, 23 adult; 43 gonadal, 11 extragonadal), 6 malignant GCT cell lines, and 21 control samples (8 teratomas and 13 gonads/yolk sac).

### MicroRNA and mRNA microarray expression analysis

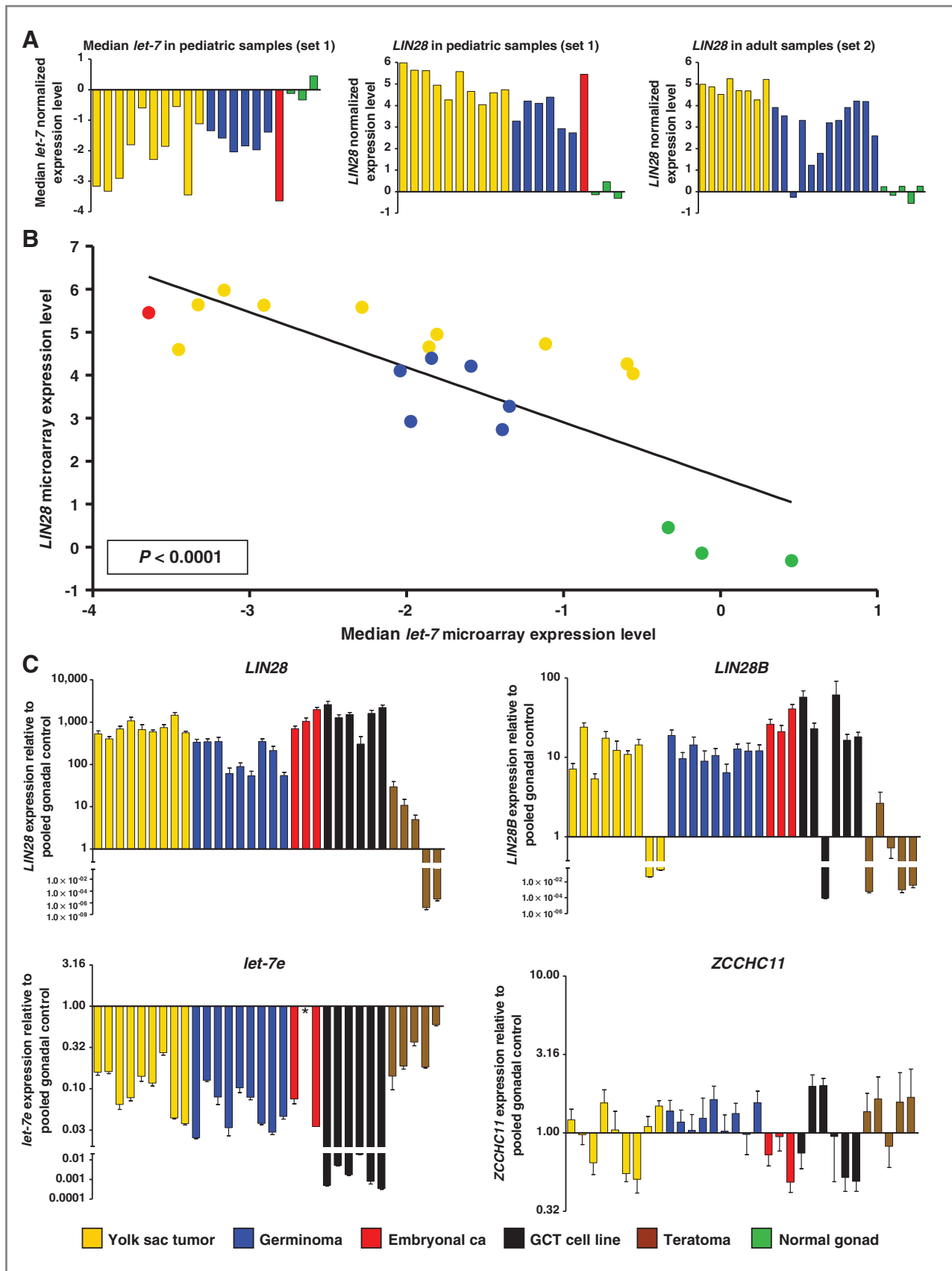
We reanalyzed microRNA expression profiles for set 1 [obtained using the miRCURY-LNA array-v9.2 (Exiqon); ref. 3] and mRNA expression profiles for sets 1 and 2 [obtained using the HG-U133A GeneChip (Affymetrix); refs. 3, 22]. Differential gene expression was assessed using a moderated *t* statistic and *P* values adjusted for multiple testing using Benjamini and Hochberg method (23). MicroRNAs with adjusted *P* values less than 0.01 were considered to be significantly differentially expressed, whereas mRNAs with  $\log_2$  fold-change 1.5 or more and adjusted *P* < 0.01 were considered to be overexpressed (3).

### Sylamer bioinformatic algorithm

*Sylamer* assesses enrichment and/or depletion of SCR nucleotide words of specific length in the 3'UTRs of genes within ranked lists (24). We used *Sylamer* to identify whether the *let-7* downregulation in malignant GCTs was of biologic significance by causing shifts in expression of mRNAs with a 3'UTR *let-7* SCR (3). We conducted 3 analyses of mRNA microarray data, examining the pediatric samples from set 1 with matched microRNA and mRNA profiles ( $n = 20$ ), the adult samples from set 2 ( $n = 25$ ), and both groups in combination ( $n = 45$ ). In *Sylamer* landscape plots, mRNA gene lists were ranked on the *x*-axis from downregulated (left) to upregulated (right). The *y*-axis showed  $\log_{10}$ -transformed and sign-adjusted enrichment *P* values for each SCR word, relative to *P* values of all other words. Consequently, an SCR showing a negative *y*-axis deflection on the right-hand side of each plot was enriched in upregulated genes. As previously (3), we calculated a single summed significance score and *P* value for each SCR. We only considered SCR elements that contained the core 2 to 7 nt sequence of the microRNA seed region, summing data for 1 hexamer (2–7 nt), 2 heptamers (1–7 nt and 2–8 nt), and 1 octamer (1–8 nt). *P* values less than 0.01 were considered significant (3). We tested for enrichment in the upregulated genes of 3'UTR SCRs corresponding to the 1 to 8 nt seeds of all 126 microRNAs downregulated in the 48 set 1 pediatric malignant GCTs (3).

### mRNA qRT-PCR

Relative mRNA transcript levels were measured in triplicate in clinical samples and cell lines using QuantiTect One-Step SYBR-Green qRT-PCR (Qiagen), following reverse transcription of 1  $\mu$ g of total RNA using QuantiTect Reverse Transcription (Qiagen). Primers (Supplementary Table S2) were designed using Primer3 (25), ensuring that they crossed exon–exon boundaries. Expression ratios were calculated using the comparative threshold cycle ( $C_t$ ) method (26) and



normalized using 4 housekeeping genes *ACTB* (Qiagen), *YWHAZ*, *RPL13A*, and *HMBS* (27). In analyses of clinical samples, results were referenced to a pooled normal gonadal control, using total RNA from human ovaries and testes (AM6974/AM7972, Ambion). It should be noted that these tissues contain both germ cells and somatic cells. For cell lines, results were referenced to cells treated with either nontargeting control (NTC) siRNA, or mimic negative control (MNC) RNA, as appropriate.

#### qRT-PCR for microRNA and pri-microRNA

MicroRNA levels were quantified in triplicate using TaqMan assays (Applied Biosystems), as described in references (3, 28). Levels of pri-microRNA were determined in quadruplicate, using TURBO DNA-free, TaqMan High Capacity RNA-to-cDNA, and TaqMan assays (all Applied Biosystems). Expression ratios were calculated using the comparative Ct method, with microRNAs normalized to *RNU24* (3, 28) and pri-microRNAs to *RPL0*, *GUS-B*, and *18S*. Reference samples were as for mRNA qRT-PCR. In test amplifications using 0.01 nmol/L single-stranded *let-7e* RNA (Sigma Aldrich) TaqMan qRT-PCR for *let-7b* and *let-7d* showed no cross-reactivity with *let-7e* (data not shown).

#### Western blotting

Western blots were conducted for LIN28, LIN28B, AURKB, and MYCN proteins using the antibodies ab46020 (1:10,000 dilution), ab119367 (1:1,000), ab2254 (1:5,000), and ab16898 (1:250), respectively. Results were normalized to  $\beta$ -tubulin (ab6046; 1:10,000). All antibodies were from Abcam. Western blot densitometry was conducted using FluorChem-9900 imaging system software (Alpha Innotech).

#### GCT cell lines

We selected four cell lines that reflected the range of malignant GCT histologic subtypes commonly observed in clinical practice, namely embryonal carcinoma (2102Ep; ref. 29), YST (GCT44 and 1411H), and germinoma/seminoma (TCam2; ref. 30). Cells were cultured at 37°C in 5% CO<sub>2</sub> in medium containing 10% fetal calf serum and 1% penicillin/streptomycin, and were authenticated using short tandem repeat profiling (3).

#### RNA depletion and overexpression

Transcripts were depleted by RNAi in overexpressing malignant GCT cell lines using pools of 4 separate siRNAs to reduce any off-target effects (31). The probes targeted *LIN28* (L-018411-01), *LIN28B* (L-028584-01), and *MYCN* (L-003913-01; all Dharmacon). Each pool was used at 66.7 nmol/L, which represented the minimal concentration of *LIN28* siRNAs that achieved more than 75% *LIN28* transcript depletion in test experiments (data not shown). All results were normalized to cells treated with a 66.7 nmol/L pool of 4 NTC siRNAs

(D-001810-10-05, Dharmacon; ref. 32). We confirmed the specific effects of the *LIN28*-targeting pool using 2 independent siRNAs (Hs\_LIN28\_7 and Hs\_LIN28\_8, both Qiagen; target sequences TAAAGACTTATTGGTACGCAA and CACGCTGTGAGATCACCGCAA, respectively). Differences between experimental observations were assessed using an unpaired, 2-sample *t* test (2-tailed with 95% confidence intervals). *Let-7e* was replenished in underexpressing malignant GCT cell lines using *let-7e* miRIDIAN double-stranded RNA-mimic (C-300479-05) at 100 nmol/L (33) and was normalized to cells treated with 100 nmol/L miRIDIAN MNC (CN-001000-01, both Dharmacon).

#### Cell transfection and proliferation assays

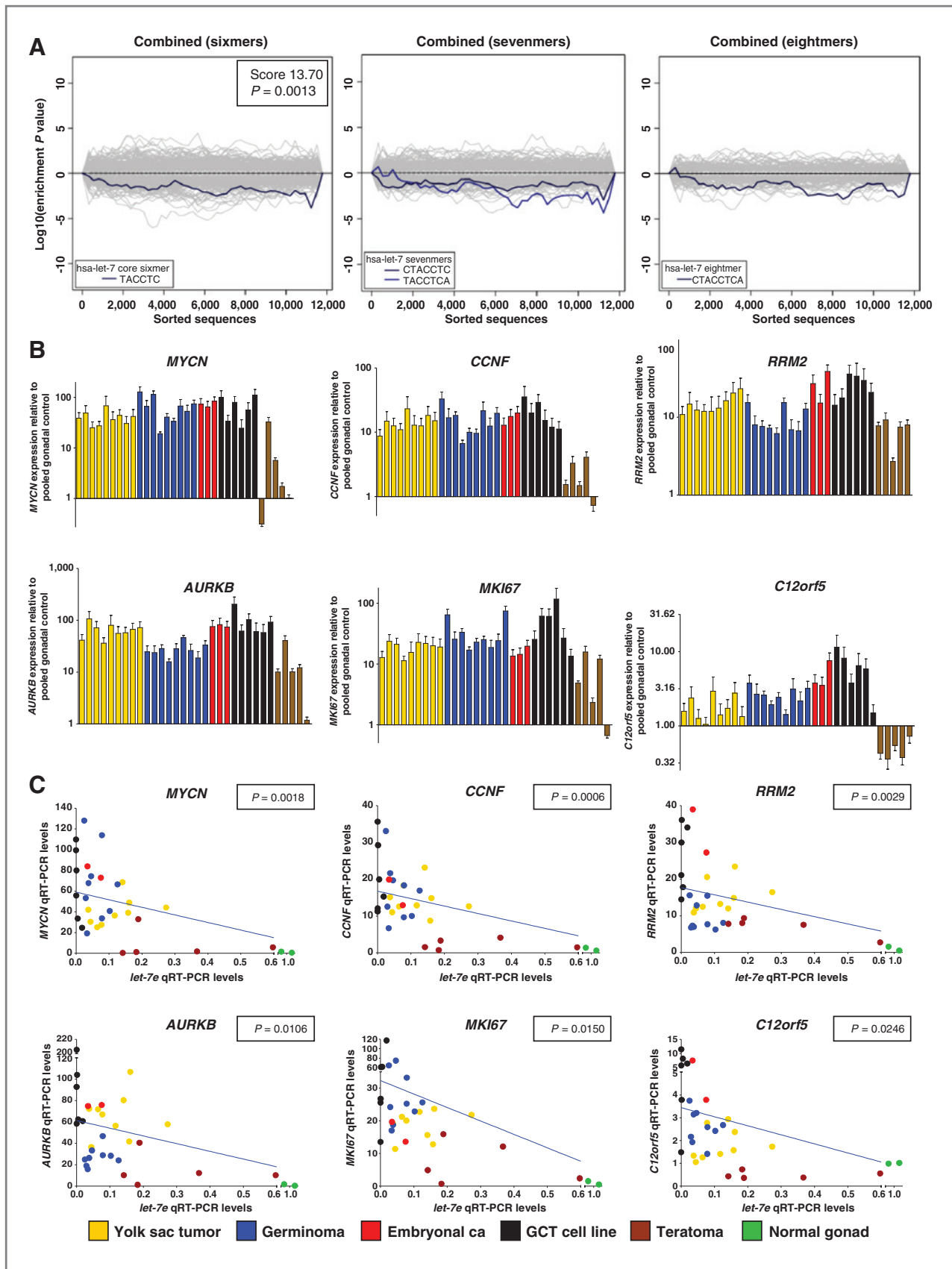
Following optimization of transfection conditions (data not shown), cells were seeded in 6-well plates, with 2102Ep at  $7 \times 10^4$  cells per well, 1411H and GCT44 at  $1.0 \times 10^5$  cells per well, and TCam2  $1.5 \times 10^5$  cells per well. On day 0 (d0), when cells were approximately 20% confluent, transfection was conducted using Opti-MEM media and Lipofectamine-RNAiMAX (both Invitrogen). The optimal length of transfection, which maximized transfection efficiency and minimized toxicity, was 24 hours for 2102Ep cell line, 6 to 8 hours for 1411H and GCT44, and 4 to 6 hours for TCam2. At least three biologic replicates were done for each treatment. For RNA and protein quantification, the replicate samples were pooled prior to further analysis. For qRT-PCR, at least three technical replicates were done per analysis.

Cell numbers were quantified using Trypan blue on a Countess automated cell counter (Invitrogen), determining the mean of two values for each of three biologic replicates and then taking the mean of the resulting three values. Maximal growth rates were determined by plotting cell numbers at 24-hour time-points on a logarithmic scale and calculating population doubling-time from the linear section of the curve, as described (34).

#### Luciferase reporter assays

We studied *let-7* effects on target genes using GoClone luciferase reporter plasmids containing the full-length 3'UTR for *LIN28* (S813978), *MYCN* (S807230), or *AURKB* (custom-made), plus a control luciferase plasmid containing no 3'UTR (S890005; all plasmids from SwitchGear Genomics). Test oligonucleotides were *let-7e*, nontargeting RNA (NT2; MIM9002), and a mutant *let-7e* (*let-7e-mutant*; sequence UGAGUGAGGAGGUGUAUAGUU), in which the 2 to 7 nt seed was mutated to "GAGUGA." The latter sequence did not correspond to any known human microRNA seed, thereby avoiding seed-like off-target effects in transfected cells. All experiments were done twice in quadruplicate in 96-well plates, using more than 80% confluent cells, with 50 ng of plasmid per well and 100 nmol/L oligonucleotides. Luminescence was quantified on a BioTek Synergy-HT multi-mode microplate reader (BioTek

**Figure 1.** *Let-7* and *LIN28* expression in malignant GCTs. A, left and middle, show median levels of all 9 *let-7* family members and levels of *LIN28* in the 20 samples from set 1 with matching microRNA and mRNA data, respectively. Right, levels of *LIN28* in sample set 2. B, linear-regression analysis of median *let-7* family levels versus *LIN28* levels in the set 1 samples with matching data. In A and B, all values are referenced to the mean of the normal gonadal samples. C, qRT-PCR validation in sample set 3, referenced to the pooled normal gonadal control sample. Error bars, SEM. For one sample (\*), there was insufficient RNA for *let-7e* quantification. The color code for all panels is shown in the key. For details of the normal gonadal controls, see Materials and Methods.



Instruments Inc). After background correction, the means for the test *let-7e/let-7e-mutant* oligonucleotides were normalized to values for NT2-treated cells, then referenced to cells containing the no 3'UTR control reporter that had also been treated with *let-7e/let-7e-mutant*, as appropriate.

## Results

### Let-7 and LIN28 expression in malignant GCTs

In our previous microRNA profiling study of sample set 1, we identified that all 9 members of the tumor-suppressor *let-7* microRNA family were significantly downregulated in pediatric malignant GCTs, compared with nonmalignant tissues (benign GCTs and normal gonad; ref. 3), which contain a variable representation of germ cells and somatic cells. The fold changes observed for each *let-7* family member are given in Supplementary Table S3, with *let-7e* being the most significantly underexpressed by *P* value. For the subset of 20 pediatric samples with matched microRNA and mRNA profiles, the malignant GCTs again showed significant reductions in *let-7* microRNAs, when assessing each family member individually (Supplementary Fig. S1A), or collectively (Fig. 1A).

As individual *let-7* members are transcribed from multiple genomic loci, this observation suggested the possibility of a common posttranscriptional mechanism regulating *let-7* biogenesis in malignant GCTs. We therefore sought to identify whether *let-7* downregulation was associated with overexpression of *LIN28*. Using all available mRNA microarray data, we found that *LIN28* was highly expressed in 44 of 45 (97.8%) of malignant GCTs from pediatric and adult patients (from sets 1 and 2 combined; Fig. 1A), regardless of tumor site (gonadal/extragenital) or histologic subtype. For the 20 pediatric samples with matched microRNA and mRNA data, *LIN28* showed a highly significant negative correlation with median *let-7* levels ( $R^2 = 0.63$ ;  $P < 0.0001$ ; Fig. 1B) and with levels of each individual *let-7* family member (all  $P < 0.005$ ; Supplementary Fig. S1B).

We validated these microarray findings using the independent technique of qRT-PCR in a panel of 32 samples (set 3). Compared with pooled normal gonadal control RNA, all 27 of the malignant GCT samples and cell lines showed high *LIN28* expression (Fig. 1C). Twenty-four of the 27 also showed high expression of *LIN28B* (Fig. 1C), which is located at a different chromosomal locus (6q16.3; vs. 1p36.11 for *LIN28*). In contrast, levels of the TUTase *ZCCHC11* were not elevated either in malignant GCT samples or teratomas (Fig. 1C). Using TaqMan qRT-PCR, we confirmed that *let-7e* (the most significantly downregulated *let-7* in our microarray analysis) showed low expression in all the malignant GCT samples/cell lines (Fig. 1C). Linear regression using the qRT-PCR data confirmed that *let-7e* levels were significantly negatively correlated with *LIN28*

and *LIN28B* ( $P = 0.017$  and  $P = 0.036$ , respectively; Supplementary Fig. S2), but not with *ZCCHC11*.

### Biologic significance of low let-7 levels in malignant GCTs

*Sylamer* showed that "TACCTC" (complementary to the 2–7 nt common *let-7* seed "GAGGUA") was the top-ranking SCR in mRNAs that significantly upregulated in malignant GCTs (compared with the normal gonadal control tissues), irrespective of patient age. There were highly significant *P* values for the summed significance scores of the *let-7* 1 to 8 nt SCR in the datasets for the pediatric malignant GCTs (set 1;  $P = 0.00057$ ), the adult malignant GCTs (set 2;  $P = 0.00026$ ; both Supplementary Fig. S3), and the combined analysis ( $P = 0.0013$ ; Fig. 2A). In all analyses, there was no significant enrichment in the upregulated mRNAs of SCRs for any of the other 126 microRNAs tested.

We used *Sylamer* to produce a list of *let-7* mRNA targets that were overexpressed in all malignant GCTs, for further validation in clinical samples and functional investigation *in vitro*. We identified 198 upregulated genes from the pediatric mRNA dataset (set 1), of which 50 (25.3%) had at least one "TACCTC" 3'UTR sequence. For the adult dataset (set 2), we identified 428 upregulated genes, of which 106 (24.8%) contained at least one 3'UTR TACCTC. These values compared with an overall frequency of 19.8% for the TACCTC sequence in the 3'UTR of all annotated genes on the array. Thirty-six *let-7* mRNA targets were common to both datasets, with 27 having a significant negative correlation with median *let-7* levels in the 20 pediatric tissue samples from set 1 that had matched microRNA and mRNA microarray data (Supplementary Table S4 and Supplementary Fig. S4). We selected 16 of these 27 genes for further interrogation, based on their reported functions in human disease, including cancer. The genes were: *MYCN*, *CCNF*, *RRM2*, *AURKB*, *MKI67*, *C12orf5*, *FZD5*, *KRAS*, *PGK1*, *SMAGP*, *RAB25*, *RAB15*, *MRS2*, *SLC2A3*, *LASPI*, and *AGL*.

*HMGA2*, a known *let-7* target in carcinoma cells (35), was included in the initial list of 36 mRNAs, as it was upregulated in both pediatric set 1 (rank 40/50) and adult set 2 (rank 63/106). However, *HMGA2* showed no significant correlation with median *let-7* levels across these datasets ( $P = 0.12$ ). To investigate these observations further, we measured *HMGA2* levels in set 3 using qRT-PCR. This showed that while *HMGA2* was overexpressed in some subtypes of malignant GCT (YSTs and embryonal carcinoma), it showed only minimal expression changes in another major subtype, germinoma (Supplementary Fig. S5A and S5B). The lack of overall association between *HMGA2* and *let-7* levels was also confirmed in this qRT-PCR analysis ( $P = 0.12$ ; Supplementary Fig. S5C).

**Figure 2.** Significance of *let-7* downregulation in malignant GCTs. A, *Sylamer* landscape plots for SCR words corresponding to the common seed of the 9 *let-7* microRNA family members in the combined analysis of pediatric (set 1) and adult (set 2) malignant GCTs. Log<sub>10</sub>-transformed *P* values for each SCR word are plotted on the y-axis, against the ranked gene list on the x-axis. A negative y-axis deflection on the right-hand side of the plot signifies SCR enrichment in upregulated genes. The left-hand plot shows data for the hexamer complementary to the core 2 to 7 nt component of the common seed region, the central plot the 2 heptamers (1–7 nt; 2–8 nt), and the right-hand plot the octamer (1–8 nt). The single summed significance score and *P* value for all 4 SCR words is shown. B, levels of the 6 selected *let-7* mRNA targets in sample set 3 determined by qRT-PCR. Error bars, SEM. C, correlations between each mRNA and *let-7e* in set 3. *P* values were determined by linear regression.

### Validation of *let-7* mRNA targets

By qRT-PCR analysis of the 32 samples in set 3, we confirmed overexpression of all 16 selected mRNAs in malignant GCTs, compared with the control samples used (Fig. 2B, Supplementary Fig. S6). We identified a negative association with *let-7e* qRT-PCR levels for 6 mRNAs (*MYCN*, *AURKB*, *CCNF*, *RRM2*, *MKI67*, and *C12orf5*; Supplementary Table S5; Fig. 2C). It should be noted that the associations were only significant when including the control samples, in which there was a mixture of germ cells and somatic cells. Accordingly, these findings should be viewed with caution in the absence of follow-up functional data (see below). On the other hand, there was no significant association for the other 10 of the 16 genes, when the control samples were included. Of these other 10 mRNAs, *RAB25*, *MRS2*, *PGKI*, *KRAS*, and *LASPI* were overexpressed in malignant GCTs of particular histologic subtypes (Supplementary Fig. S6), but did not show an association with *let-7e* levels across the whole sample set. The other 5 mRNAs (*FZD5*, *SMAGP*, *RAB15*, *SLC2A3*, and *AGL*) showed no association with *let-7e* qRT-PCR levels (Supplementary Fig. S6), suggesting that their expression is regulated by additional factors, which may include other microRNAs.

### Depletion of *LIN28* and *LIN28B*

We next tested the functional significance of our observations *in vitro*, using multiple complementary experimental approaches to minimize the possibility of nonspecific observations. We tested for phenotypic and functional consistencies when: (i) depleting *LIN28* or *LIN28B* by RNAi, using panels of 4 siRNAs to minimize any off-target effects (31), with separate confirmation using independent siRNAs; (ii) directly overexpressing *let-7e* (the *let-7* family member that showed the most significant underexpression *in vivo*; Supplementary Table S3) using a double-stranded RNA mimic; and (iii) depleting *MYCN*, a major *let-7e* target, by RNAi using a panel of 4 independent siRNAs. In this *in vitro* work, we used 4 representative malignant GCT cell lines, all of which showed *LIN28* upregulation and *let-7* underexpression (Fig. 1C).

In 2102Ep cells, a single treatment with pooled siRNAs depleted *LIN28* mRNA by more than 90% over a 7-day period. There were parallel reductions in protein levels, which fell to less than 10% from d3 (Fig. 3A and Supplementary Fig. S7A). There was no effect on *LIN28B* or *ZCCHC11* mRNA levels on d1 to d3 (data not shown). The reductions in *LIN28* protein levels were mirrored by changes in cell proliferation, which fell from d3 (Fig. 3B). There was a 36% increase in mean population doubling time over the 7d time-course (33.9 vs. 24.9 hours, respectively).

In keeping with these observations, levels of *let-7e* started increasing from d3, with significant changes from d4 (Fig. 3C). The specificity of the effects of the pooled *LIN28* siRNAs on cell proliferation and *let-7e* levels was confirmed using 2 independent siRNAs (Supplementary Fig. S8). The pooled *LIN28* siRNAs also caused increases in other representative *let-7* family members (*let-7b* and *let-7d*), when assessed at d4 and d7 (Fig. 3D). There was no difference in levels of the *pri-let-7e* precursor at d7 (data not shown). Of the selected *let-7* mRNA targets (Fig. 2B), all 6 showed decreased levels on d4 and d7 (time-points at

which growth-inhibition was observed), compared with d2 (when no growth-inhibition was seen). Most of the decreases were statistically significant (Fig. 3D), with the most significant reduction being for *MYCN*, where transcript levels were lowered by 62% at d4 versus d2 ( $P < 0.0001$ ; Fig. 3D).

We attempted to deplete *LIN28* in 3 other malignant GCT cell lines, assessing the effects at d4 posttransfection, based on our findings in 2102Ep. While we could achieve 87% transcript depletion in TCam2, cell toxicity restricted the levels of depletion achieved in 1411H and GCT44 to 57% and 46%, respectively. There were parallel reductions in protein levels, as measured at d4 following siRNA treatment (Supplementary Fig. S7B), with a significant positive correlation between *LIN28* mRNA and protein levels across the 4 cell lines ( $R^2 = 0.88$ ,  $P < 0.0001$ ; Supplementary Fig. S7C). The *LIN28* reductions observed in 1411H and GCT44 were not sufficient to affect cell numbers, compared with NTC-treated cells (Fig. 4A and Supplementary Fig. S7D). However, across all 4 cell lines, there were significant positive correlations between levels of *LIN28* and *MYCN* transcripts ( $R^2 = 0.78$ ,  $P = 0.0001$ ; Fig. 4B) and between cell proliferation (quantifying cell numbers at d4) and transcript levels of *LIN28* ( $R^2 = 0.85$ ,  $P < 0.0001$ ) and *MYCN* ( $R^2 = 0.78$ ,  $P < 0.0001$ ; Fig. 4A).

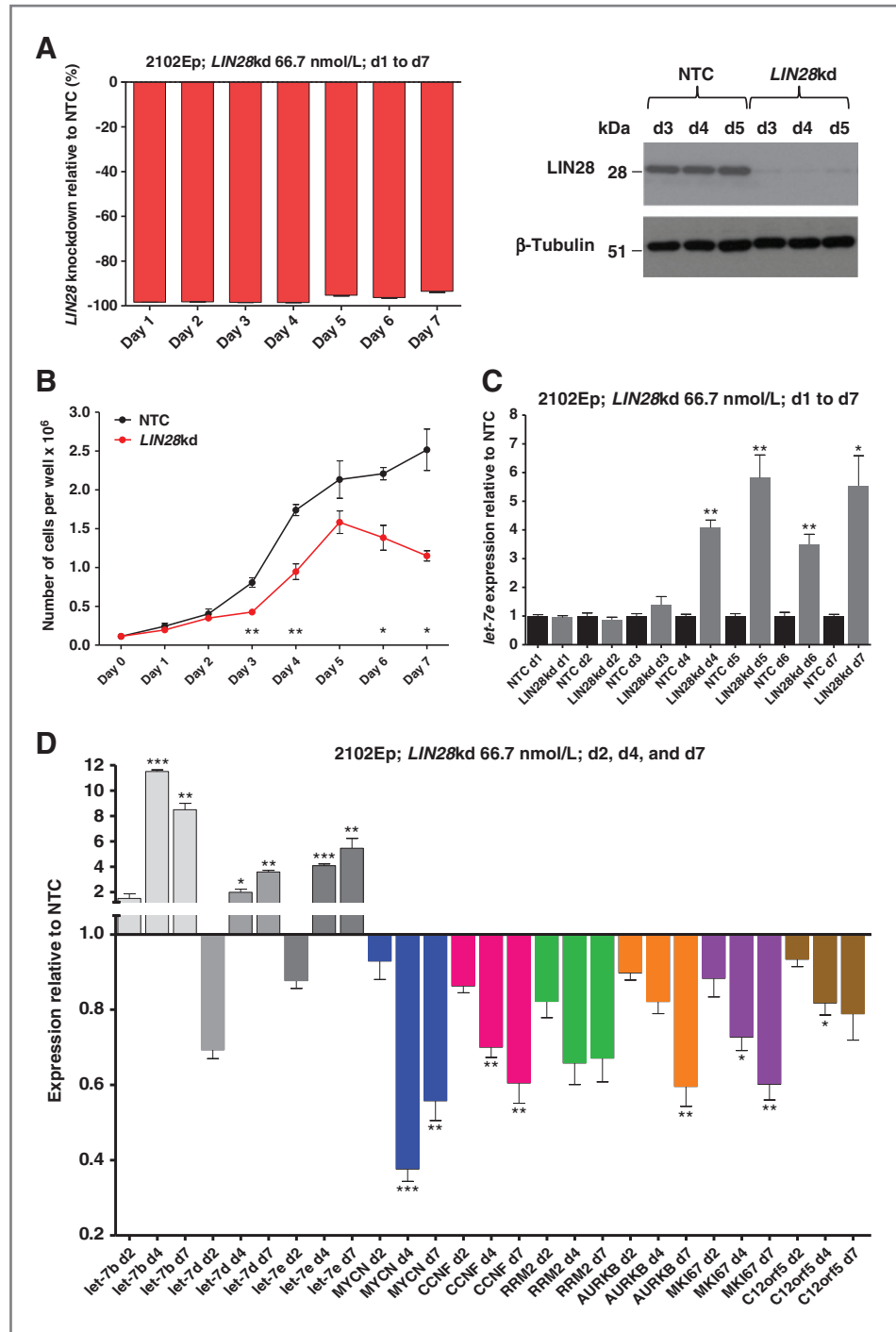
We next depleted *LIN28B* in 2102Ep and TCam2, achieving more than 80% transcript depletion and more than 85% protein depletion by d4 (Fig. 5A and B). In contrast to the effects of *LIN28* depletion (Fig. 3D), we observed only modest increases in levels of *let-7b*, *let-7d*, and *let-7e* (1.21–1.96-fold; Fig. 5C), with no effect on *MYCN* levels or cell proliferation (Fig. 5A).

### Restoration of *let-7* levels

Transfection with *let-7e* mimic produced the greatest increases in *let-7e* levels in 2102Ep and 1411H (Fig. 6), which were selected for further investigations. In both cell lines, *let-7e* transfection resulted in significant reductions in mRNA levels of *MYCN* and *LIN28* at d2, when compared with MNC-treated cells (all  $P \leq 0.001$ ; Fig. 6A). Over a 3d time-course in 2102Ep, we observed reduced levels of *MYCN*, *AURKB*, *LIN28*, and *LIN28B* transcripts (Supplementary Fig. S9A), with a significant negative correlation between mean transcript depletion over d1 to d3 and the number of 3'UTR *let-7* SCRs ( $R^2 = 0.97$ ,  $P = 0.0145$ ; Supplementary Fig. S9B). Levels of all 4 proteins were reduced when assessed on d2 and d3 (Fig. 6B and C). Overall, across the 4 malignant GCT cell lines examined, there was a significant negative correlation between *let-7e* levels obtained following *let-7e* mimic transfection and cell proliferation ( $R^2 = 0.94$ ;  $P < 0.0001$ ; Fig. 6D).

The *LIN28* and *LIN28B* depletion (Fig. 6A, Supplementary Fig. S9A) were explained by the presence in 3'UTRs of the "TACCTC" SCR for the common 2 to 7 nt *let-7* seed, with one copy in *LIN28* (Supplementary Fig. S9C) and 5 copies in *LIN28B* (data not shown). In keeping with the reduced *LIN28* levels, we observed approximately 15- to 30-fold increases in other *let-7* family members examined (*let-7b* and *let-7d*) in both 2102Ep ( $P = 0.0001$  for both) and 1411H ( $P = 0.0006$  and  $P = 0.0002$ , respectively; Fig. 6E). There was no increase in levels of a control microRNA (miR-492) lacking the *LIN28* "GGAG" binding site in its stem-loop (Fig. 6E).

**Figure 3.** LIN28 depletion in 2102Ep malignant GCT cells. A, depletion of LIN28, measured by qRT-PCR over d1–d7 (left) and by Western blot analysis over d3–d5 (right). NTC, nontargeting control siRNA; kd, knockdown. B, cell numbers following LIN28 depletion. C, levels of *let-7e* more than d1–d7 following LIN28 depletion. A–C, statistical comparisons are versus NTC-treated cells. d, day. D, levels of *let-7* family members (*let-7b*, *let-7d*, and *let-7e*) and the 6 selected *let-7* mRNA targets at d2, d4, and d7 following LIN28 depletion. Expression values are referenced to NTC-treated cells. Statistical comparisons are for LIN28kd cells at d4 and d7 versus LIN28kd cells at d2. Error bars, SEM. B–D, \*,  $P < 0.05$ ; \*\*,  $P < 0.005$ ; \*\*\*,  $P \leq 0.0001$ .



We confirmed *let-7e* effects on *LIN28*, *MYCN*, and *AURKB* using quantitative luciferase reporter assays. *Let-7e* produced a significant reduction in luminescence relative to nontargeting oligonucleotides, in cells containing the 3'UTR for *LIN28* ( $P = 0.0003$ ), *MYCN* ( $P = 0.011$ ) or *AURKB* ( $P < 0.0001$ ), whereas there were no reductions with mutant *let-7e* (Fig. 7). These findings are supported by evidence from other cell types showing direct targeting of *MYCN* by *let-7e* (36) and

of *AURKB* by *let-7b* (37), which has an identical 2 to 7 nt seed to that of *let-7e*.

**Effects of MYCN depletion**

We tested whether *LIN28/LIN28B* levels in malignant GCTs might be regulated by *MYCN* and the related protein *CMYC*, similar to findings in other tumor types (38, 39). Our microarray data showed upregulation of *MYCN* in both pediatric (set

Downloaded from http://aacrjournals.org/cancerres/article-pdf/73/15/4872/206941154872.pdf by guest on 26 May 2024



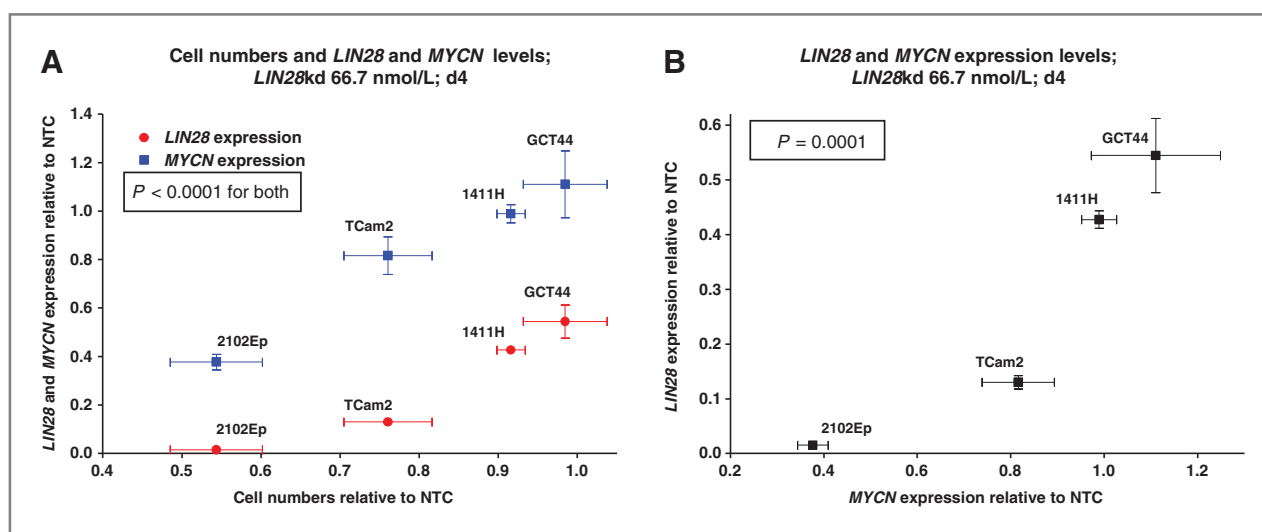


**Figure 4.** Correlations between *LIN28*, *MYCN*, and cell numbers following *LIN28* depletion. The graphs show data for all 4 malignant GCT cell lines at d4 following *LIN28* depletion, compared with NTC-treated cells. A and B, cell numbers versus the levels of *LIN28* (red) and *MYCN* (blue; A), whereas B shows levels of *MYCN* versus *LIN28* (B). NTC, nontargeting control siRNA; kd, knockdown. Correlation  $P$  values were determined by linear regression. Error bars, SEM.

1;  $n = 20$ ) and adult (set 2;  $n = 25$ ) malignant GCTs, compared with the controls used. There was a significant positive correlation with *LIN28* levels in both sets ( $P < 0.0001$  and  $P = 0.001$ , respectively; Supplementary Fig. S10). In contrast, *CMYC* levels showed no elevation and no positive correlation with *LIN28* in either set (Supplementary Fig. S10). As *LIN28B* was not represented on the microarray used to profile mRNAs in the pediatric malignant GCTs, we used qRT-PCR analysis of set 3 ( $n = 32$ ) to show significant positive correlations between *MYCN* and both *LIN28* and *LIN28B* in malignant GCTs ( $P = 0.0018$  and  $P = 0.0121$ , respectively). While depleting *MYCN* in 2102Ep and TCam2 reduced cell numbers, it had no consistent effects on levels of *LIN28* or *LIN28B* (Supplementary Fig. S11). Together, these data supported our evidence that *MYCN* is an important upregulated *let-7* target in malignant GCT cells, but argued against a significant effect of *MYCN* or *CMYC* upstream of *LIN28/LIN28B*.

## Discussion

This study shows that *LIN28-homolog A* (*LIN28*) is abundantly expressed in all malignant GCTs, regardless of patient age, histologic type or anatomic site, thereby extending published reports describing predominantly or exclusively tumors of adults (17–20). Importantly, we identify the functional significance of the observed *LIN28* expression, which results in *let-7* family downregulation (Supplementary Fig. S12). Our qRT-PCR analysis of tissue samples suggested that *let-7* under-expression may contribute to increased expression of *let-7* protein-coding gene targets, a possibility that was supported by our functional data from *LIN28* depletion and *let-7e* over-expression experiments. The potential *let-7* targets in malignant GCTs have known promalignant effects, such as increased proliferation and reduced apoptosis (Supplementary Table S5). While *LIN28B* is also highly expressed in malignant GCTs, our data do not indicate an important role for the protein in regulating *let-7* microRNAs.

A previous study showed that *LIN28* depletion in malignant GCT cells led to downregulation of stem-cell markers (e.g., *OCT4/POU5F1* and *NANOG*) and induction of differentiation, although effects on *let-7* expression were not assessed (20). In our *LIN28* depletion experiments, protein levels fell to less than 10% from d3, a change that coincided with reduced cell growth from d3 and increased *let-7* levels from d4. These findings are consistent with the observation that *LIN28* depletion in carcinoma cells *in vitro* was not associated with significant increases in *let-7* levels until d4 after transfection (40). In addition, the *let-7e* targets identified in the present study resonate with those seen in other malignancies, suggesting molecular parallels between disparate tumor types (40, 41). Posttranscriptional effects of *LIN28/let-7* deregulation on *MYCN* levels (36) would explain the observations that *MYCN* is frequently overexpressed in malignant GCTs (42) but shows copy number gain (at 2p23.4) in only approximately 1/3 of adult tumors (43) and less than 1/5 of pediatric cases (44). Interestingly, we found that *LIN28* depletion led to increased levels of mature *let-7* without reducing levels of *pri-let-7*. It is likely that levels of *pri-let-7* are low even in the presence of abundant *LIN28*, for example due to degradation after *LIN28* binding.

As well as downregulation of *let-7* by *LIN28*, we observed a reciprocal effect, with downregulation of *LIN28* by *let-7e*, via a *let-7* SCR in the *LIN28* 3'UTR (45, 46). In malignant GCT cells, *let-7e*-mediated downregulation of *LIN28* produced specific effects, by increasing other *let-7* family targets of *LIN28* rather than producing a more generalized effect on microRNA biogenesis. Other microRNAs known to downregulate *LIN28* in embryonic stem-cells and cancer cells through 3'UTR SCRs include miR-9 (47), miR-30 family (47), miR-125 (47, 48), and miR-181 (49). Interestingly, all 4 were identified in our previous profiling study as being universally underexpressed in malignant GCTs, compared with the control tissues used (3). As copy number gain at the *LIN28* locus (1p36.11) is not a feature of malignant GCTs (44), downregulation of these microRNAs is

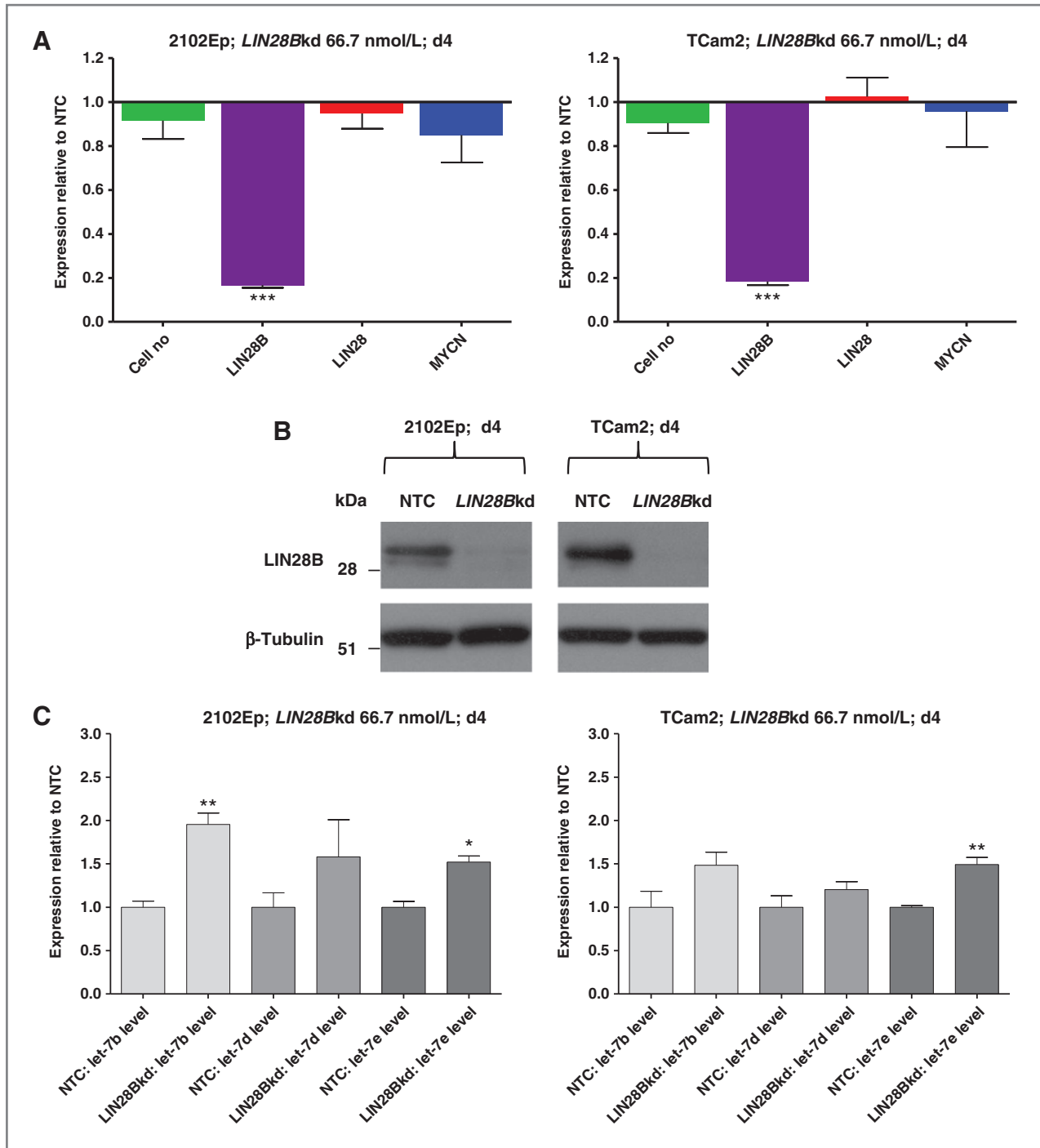


Figure 5. *LIN28B* depletion in malignant GCT cells. A, cell numbers and qRT-PCR expression levels of *LIN28B*, *LIN28*, and *MYCN* on d4 following *LIN28B* depletion in 2102Ep (left) and TCam2 (right). B, Western blots showing expression of *LIN28B* on d4 following *LIN28B* depletion in 2102Ep (left) and TCam2 (right), compared with NTC-treated cells. C, levels of representative *let-7* family members (*let-7b*, *let-7d*, and *let-7e*) on d4 following *LIN28B* depletion in 2102Ep (left) and TCam2 (right). All values are referenced to NTC-treated cells. NTC, nontargeting control siRNA; kd, knockdown; error bars, SEM. \*,  $P < 0.05$ ; \*\*,  $P < 0.005$ ; \*\*\*,  $P \leq 0.0001$ .

likely to be an important further contributor to *LIN28* overexpression *in vivo*.

Our data suggest that *LIN28/let-7* interactions are promising targets for novel therapies in malignant GCTs. As well as

directly depleting *LIN28*, it may also be possible to overcome the effects of overexpressed *LIN28* on microRNA maturation, for example, by protective small molecule targeting of *pre-let-7* stem-loop binding motifs, inhibition of the TUTase ZCCHC11,

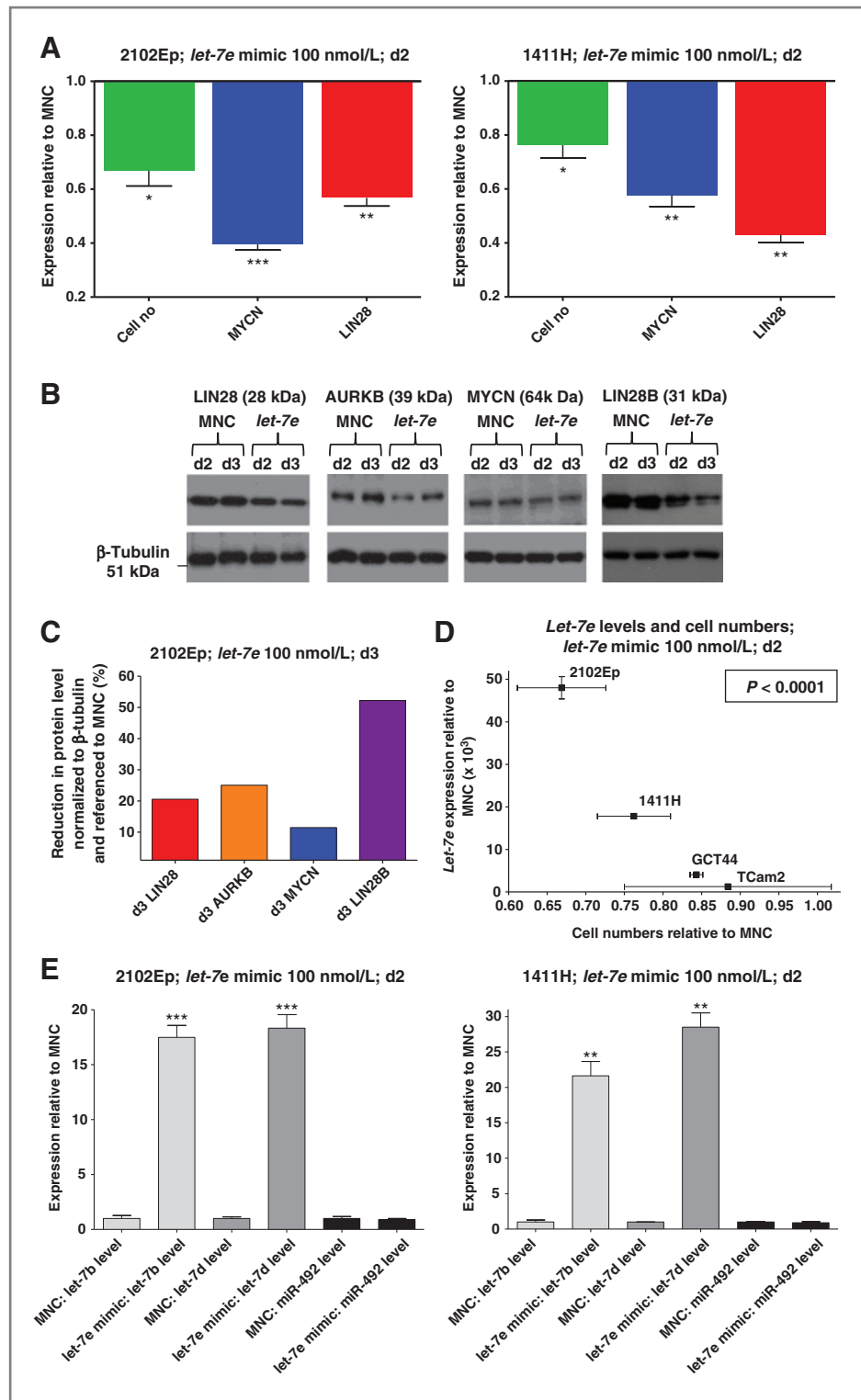
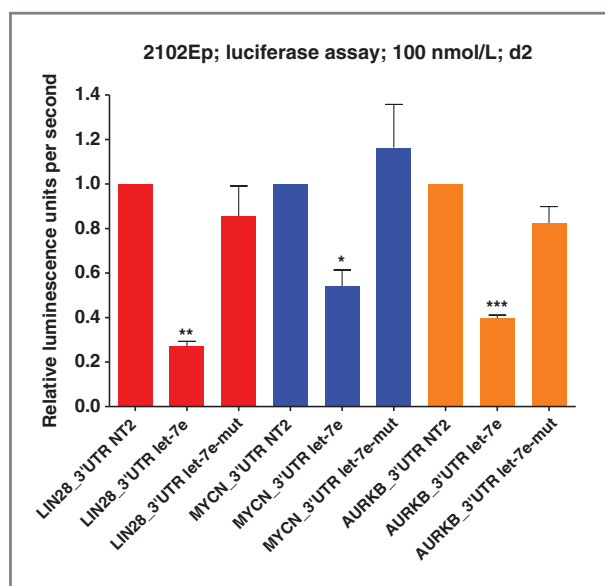


Figure 6. Effects of *let-7e* mimic in malignant GCT cells. A, cell numbers and expression levels of *MYCN* and *LIN28* in 2102Ep (left) and 1411H (right), at d2 posttransfection of *let-7e* mimic, relative to cells treated with mimic negative control (MNC) RNA. B, Western blots showing expression of *LIN28*, *AURKB*, *MYCN*, and *LIN28B* proteins at d2 and d3 following *let-7e* mimic transfection of 2102Ep cells, corresponding to Supplementary Fig. S9A. The bottom row shows the  $\beta$ -tubulin loading control. C, the graph shows protein levels at d3, as determined by densitometry of the Western blots shown in B, normalized to  $\beta$ -tubulin and referenced to MNC-treated cells. D, cell numbers versus *let-7e* levels at d2 in 4 different malignant GCT cell lines compared with MNC-treated cells. The *P* value was determined by linear regression. E, levels of other representative *let-7* family members (*let-7b* and *let-7d*) and control miR-492, at d2 following *let-7e* transfection in 2102Ep (left) and 1411H (right), relative to MNC-treated cells.

Downloaded from <http://aacrjournals.org/cancerres/article-pdf/73/15/4872/206841154872.pdf> by guest on 26 May 2024

or induction of the stem-loop binding protein KSRP, which promotes maturation of a subset of microRNAs that includes *let-7* (50). These indirect interventions would not counteract *LIN28* effects on primary transcript processing and may not

restore adequate levels of mature *let-7* molecules if used in isolation. An alternative strategy is direct replacement of *let-7* using mature *let-7* mimics. Our data indicate that administering a single member of the *let-7* family should restore



**Figure 7.** Luciferase assay confirmation of *let-7* targets in malignant GCT cells. Luciferase assay data at d2 for 2102Ep cells transfected with a reporter containing the full-length 3'UTR for *LIN28* (red), *MYCN* (blue), or *AURKB* (orange). Cells were also transfected with either *let-7e* or *let-7e-mutant* (*let-7e-mut*). Luminescence values were normalized to cells treated with nontargeting oligonucleotides (NT2), then referenced to cells containing a no 3'UTR control reporter and treated with *let-7e/let-7e-mutant*, as appropriate. Error bars, SEM. All correlation *P* values were determined by linear regression. \*, *P* < 0.05; \*\*, *P* < 0.005; \*\*\*, *P* ≤ 0.0001.

levels of other family members in malignant GCTs by targeting *LIN28*. The other *let-7* members would lead to further reinforcement of *LIN28* downregulation, providing a molecular

## References

- Murray MJ, Nicholson JC. Germ cell tumours in children and adolescents. *paediatrics and child health* 2010;20:109–16.
- Huyghe E, Matsuda T, Thonneau P. Increasing incidence of testicular cancer worldwide: a review. *J Urol* 2003;170:5–11.
- Palmer RD, Murray MJ, Saini HK, van Dongen S, Abreu-Goodger C, Muralidhar B, et al. Malignant germ cell tumors display common microRNA profiles resulting in global changes in expression of messenger RNA targets. *Cancer Res* 2010;70:2911–23.
- Lewis BP, Shih IH, Jones-Rhoades MW, Bartel DP, Burge CB. Prediction of mammalian microRNA targets. *Cell* 2003;115:787–98.
- Lewis BP, Burge CB, Bartel DP. Conserved seed pairing, often flanked by adenosines, indicates that thousands of human genes are microRNA targets. *Cell* 2005;120:15–20.
- Takamizawa J, Konishi H, Yanagisawa K, Tomida S, Osada H, Endoh H, et al. Reduced expression of the *let-7* microRNAs in human lung cancers in association with shortened postoperative survival. *Cancer Res* 2004;64:3753–6.
- Johnson CD, Esquela-Kerscher A, Stefani G, Byrom M, Kelnar K, Ovcharenko D, et al. The *let-7* microRNA represses cell proliferation pathways in human cells. *Cancer Res* 2007;67:7713–22.
- Viswanathan SR, Daley GQ, Gregory RI. Selective blockade of microRNA processing by *Lin28*. *Science* 2008;320:97–100.
- Viswanathan SR, Powers JT, Einhorn W, Hoshida Y, Ng TL, Toffanin S, et al. *Lin28* promotes transformation and is associated with advanced human malignancies. *Nat Genet* 2009;41:843–8.
- Hagan JP, Piskounova E, Gregory RI. *Lin28* recruits the TUTase *Zcchc11* to inhibit *let-7* maturation in mouse embryonic stem cells. *Nat Struct Mol Biol* 2009;16:1021–5.
- Viswanathan SR, Daley GQ. *Lin28*: A microRNA regulator with a macro role. *Cell* 2010;140:445–9.
- Heo I, Joo C, Kim YK, Ha M, Yoon MJ, Cho J, et al. *TUT4* in concert with *Lin28* suppresses microRNA biogenesis through pre-microRNA uridylation. *Cell* 2009;138:696–708.
- Loughlin FE, Gebert LF, Towbin H, Brunschweiler A, Hall J, Allain FH. Structural basis of pre-*let-7* miRNA recognition by the zinc knuckles of pluripotency factor *Lin28*. *Nat Struct Mol Biol* 2012;19:84–9.
- Heo I, Joo C, Cho J, Ha M, Han J, Kim VN. *Lin28* mediates the terminal uridylation of *let-7* precursor microRNA. *Mol Cell* 2008;32:276–84.
- Peng S, Maible NJ, Huang Y. Pluripotency factors *Lin28* and *Oct4* identify a sub-population of stem cell-like cells in ovarian cancer. *Oncogene* 2010;29:2153–9.
- West JA, Viswanathan SR, Yabuuchi A, Cunniff K, Takeuchi A, Park IH, et al. A role for *Lin28* in primordial germ-cell development and germ-cell malignancy. *Nature* 2009;460:909–13.
- Cao D, Allan RW, Cheng L, Peng Y, Guo CC, Dahiya N, et al. RNA-binding protein *LIN28* is a marker for testicular germ cell tumors. *Hum Pathol* 2011;42:710–8.
- Cao D, Liu A, Wang F, Allan RW, Mei K, Peng Y, et al. RNA-binding protein *LIN28* is a marker for primary extragonadal germ cell tumors: an immunohistochemical study of 131 cases. *Mod Pathol* 2011;24:288–96.
- Xue D, Peng Y, Wang F, Allan RW, Cao D. RNA-binding protein *LIN28* is a sensitive marker of ovarian primitive germ cell tumours. *Histopathology* 2011;59:452–9.
- Gillis AJ, Stoop H, Biermann K, van Gurp RJ, Swartzman E, Cribbes S, et al. Expression and interdependencies of pluripotency factors *LIN28*,

"switch" effect that should result in a sustained reversion of cell phenotype.

## Disclosure of Potential Conflicts of Interest

No potential conflicts of interest were disclosed.

## Authors' Contributions

**Conception and design:** M.J. Murray, C.A. Siegler, J.E. Hanning, I.J. Groves, C.G. Scarpini, A.J. Enright, J.C. Nicholson, N. Coleman

**Development of methodology:** M.J. Murray, C.A. Siegler, J.E. Hanning, I.J. Groves, C.G. Scarpini, M.R. Pett, J.C. Nicholson, N. Coleman

**Acquisition of data (provided animals, acquired and managed patients, provided facilities, etc.):** M.J. Murray, C.A. Siegler, J.E. Hanning, D.M. Ward, K.L. Raby, N. Coleman

**Analysis and interpretation of data (e.g., statistical analysis, biostatistics, computational analysis):** M.J. Murray, H.K. Saini, C.A. Siegler, J.E. Hanning, E.M. Barker, S. van Dongen, D.M. Ward, K.L. Raby, I.J. Groves, C.G. Scarpini, A.J. Enright, J.C. Nicholson, N. Coleman

**Writing, review, and/or revision of the manuscript:** M.J. Murray, H.K. Saini, J.E. Hanning, I.J. Groves, C.G. Scarpini, A.J. Enright, J.C. Nicholson, N. Coleman

**Administrative, technical, or material support (i.e., reporting or organizing data, constructing databases):** M.J. Murray, E.M. Barker, D.M. Ward, K.L. Raby, C.M. Thornton, A.J. Enright

**Study supervision:** M.J. Murray, J.C. Nicholson, N. Coleman

## Acknowledgments

The authors thank Mr Alex Byford for technical assistance.

## Grant Support

This work was supported by Cancer Research-UK programme grant (N. Coleman), Medical Research Council Fellowship (M.J. Murray), and Addenbrooke's Charitable Trust (M.J. Murray).

The costs of publication of this article were defrayed in part by the payment of page charges. This article must therefore be hereby marked advertisement in accordance with 18 U.S.C. Section 1734 solely to indicate this fact.

Received May 25, 2012; revised May 8, 2013; accepted June 10, 2013; published OnlineFirst June 17, 2013.

- OCT3/4, NANOG and SOX2 in human testicular germ cells and tumours of the testis. *Int J Androl* 2011;34:e160–74.
21. Mills SE. *Sternbergs histology for pathologists*. 3rd ed. New York: Lippincott, Williams and Wilkins; 2006.
  22. Korkola JE, Houldsworth J, Chadalavada RS, Olshen AB, Dobrzynski D, Reuter VE, et al. Down-regulation of stem cell genes, including those in a 200-kb gene cluster at 12p13.31, is associated with *in vivo* differentiation of human male germ cell tumors. *Cancer Res* 2006;66:820–7.
  23. Benjamini Y HY. Controlling the false discovery rate—a practical and powerful approach to multiple testing. *J R Stat Soc Ser B* 1995;57:289–300.
  24. van Dongen S, Abreu-Goodger C, Enright AJ. Detecting microRNA binding and siRNA off-target effects from expression data. *Nat Methods* 2008;5:1023–5.
  25. Primer 3. [cited 26th August 2012]; Available from: <http://frodo.wi.mit.edu/primer3/>
  26. Herdman MT, Pett MR, Roberts I, Alazawi WO, Teschendorff AE, Zhang XY, et al. Interferon-beta treatment of cervical keratinocytes naturally infected with human papillomavirus 16 episomes promotes rapid reduction in episome numbers and emergence of latent integrants. *Carcinogenesis* 2006;27:2341–53.
  27. Vandesompele J, De Preter K, Pattyn F, Poppe B, Van Roy N, De Paepe A, et al. Accurate normalization of real-time quantitative RT-PCR data by geometric averaging of multiple internal control genes. *Genome Biol* 2002;3:RESEARCH0034.
  28. Murray MJ, Saini HK, van Dongen S, Palmer RD, Muralidhar B, Pett MR, et al. The two most common histological subtypes of malignant germ cell tumour are distinguished by global microRNA profiles, associated with differential transcription factor expression. *Mol Cancer* 2010;9:290.
  29. Damjanov I, Andrews PW. Ultrastructural differentiation of a clonal human embryonal carcinoma cell line *in vitro*. *Cancer Res* 1983;43:2190–8.
  30. de Jong J, Stoop H, Gillis AJ, Hersmus R, van Gurp RJ, van de Geijn GJ, et al. Further characterization of the first seminoma cell line TCam-2. *Genes Chromosomes Cancer* 2008;47:185–96.
  31. Birmingham A, Anderson EM, Reynolds A, Ilsley-Tyree D, Leake D, Fedorov Y, et al. 3' UTR seed matches, but not overall identity, are associated with RNAi off-targets. *Nat Methods* 2006;3:199–204.
  32. Muralidhar B, Winder D, Murray M, Palmer R, Barbosa-Morais N, Saini H, et al. Functional evidence that Drosha overexpression in cervical squamous cell carcinoma affects cell phenotype and microRNA profiles. *J Pathol* 2011;224:496–507.
  33. Li Z, Wu F, Brant SR, Kwon JH. IL-23 receptor regulation by Let-7f in human CD4<sup>+</sup> memory T cells. *J Immunol* 2011;186:6182–90.
  34. Pett MR, Alazawi WO, Roberts I, Downen S, Smith DI, Stanley MA, et al. Acquisition of high-level chromosomal instability is associated with integration of human papillomavirus type 16 in cervical keratinocytes. *Cancer Res* 2004;64:1359–68.
  35. Boyerinas B, Park SM, Shomron N, Hedegaard MM, Vinther J, Andersen JS, et al. Identification of let-7-regulated oncofetal genes. *Cancer Res* 2008;68:2587–91.
  36. Buechner J, Tomte E, Haug BH, Henriksen JR, Lokke C, Flaegstad T, et al. Tumour-suppressor microRNAs let-7 and mir-101 target the proto-oncogene MYCN and inhibit cell proliferation in MYCN-amplified neuroblastoma. *Br J Cancer* 2011;105:296–303.
  37. Selbach M, Schwanhauser B, Thierfelder N, Fang Z, Khanin R, Rajewsky N. Widespread changes in protein synthesis induced by microRNAs. *Nature* 2008;455:58–63.
  38. Chang TC, Zeitels LR, Hwang HW, Chivukula RR, Wentzel EA, Dewes M, et al. Lin-28B transactivation is necessary for Myc-mediated let-7 repression and proliferation. *Proc Natl Acad Sci U S A* 2009;106:3384–9.
  39. Cotterman R, Knoepfler PS. N-Myc regulates expression of pluripotency genes in neuroblastoma including *lif*, *klf2*, *klf4*, and *lin28b*. *PLoS ONE* 2009;4:e5799.
  40. Helland A, Anglesio MS, George J, Cowin PA, Johnstone CN, House CM, et al. Deregulation of MYCN, LIN28B and LET7 in a molecular subtype of aggressive high-grade serous ovarian cancers. *PLoS ONE* 2011;6:e18064.
  41. Molenaar JJ, Domingo-Fernandez R, Ebus ME, Lindner S, Koster J, Drabek K, et al. LIN28B induces neuroblastoma and enhances MYCN levels via let-7 suppression. *Nat Genet* 2012;44:1199–206.
  42. Alagaratnam S, Lind GE, Kraggerud SM, Lothe RA, Skotheim RI. The testicular germ cell tumour transcriptome. *Int J Androl* 2011;34:e133–50; discussion e50–1.
  43. Kraggerud SM, Skotheim RI, Szymanska J, Eknaes M, Fossa SD, Stenwig AE, et al. Genome profiles of familial/bilateral and sporadic testicular germ cell tumors. *Genes Chromosomes Cancer* 2002;34:168–74.
  44. Palmer RD, Foster NA, Vowler SL, Roberts I, Thornton CM, Hale JP, et al. Malignant germ cell tumours of childhood: new associations of genomic imbalance. *Br J Cancer* 2007;96:667–76.
  45. Chen AX, Yu KD, Fan L, Li JY, Yang C, Huang AJ, et al. Germline genetic variants disturbing the Let-7/LIN28 double-negative feedback loop alter breast cancer susceptibility. *PLoS Genet* 2011;7:e1002259.
  46. Yang X, Lin X, Zhong X, Kaur S, Li N, Liang S, et al. Double-negative feedback loop between reprogramming factor LIN28 and microRNA let-7 regulates aldehyde dehydrogenase 1-positive cancer stem cells. *Cancer Res* 2010;70:9463–72.
  47. Zhong X, Li N, Liang S, Huang Q, Coukos G, Zhang L. Identification of microRNAs regulating reprogramming factor LIN28 in embryonic stem cells and cancer cells. *J Biol Chem* 2010;285:41961–71.
  48. Wu L, Belasco JG. Micro-RNA regulation of the mammalian lin-28 gene during neuronal differentiation of embryonal carcinoma cells. *Mol Cell Biol* 2005;25:9198–208.
  49. Li X, Zhang J, Gao L, McClellan S, Finan MA, Butler TW, et al. MiR-181 mediates cell differentiation by interrupting the Lin28 and let-7 feedback circuit. *Cell Death Differ* 2012;19:378–86.
  50. Trabucchi M, Briata P, Garcia-Mayoral M, Haase AD, Filipowicz W, Ramos A, et al. The RNA-binding protein KSRP promotes the biogenesis of a subset of microRNAs. *Nature* 2009;459:1010–4.